Supplementary information

Bimetallic ruthenium-rhodium particles supported on carbon nanotubes for the hydrophosphinylation of alkenes and alkynes

Dhanaji V. Jawale, Frédéric Fossard, Frédéric Miserque, Valérie Geertsen, Eric Doris and Edmond Gravel

Table of contents

1. General

Chemicals and solvents were purchased from commercial suppliers. Flash chromatography was carried out on Kieselgel 60 (230–240 mesh, Merck) and analytical TLC was performed on Merck precoated silica gel (60 F254). Compounds were visualized under UV light and/or by treatment with a solution of phosphomolybdic acid in ethanol followed by heating. NMR spectra were recorded on a Bruker Avance spectrometer at 400 MHz (^{1}H), 100 MHz (^{13}C). Chemical shifts are given in ppm relative to the NMR solvent residual peak, coupling constants *J* are given in Hz. Unless otherwise specified, ultrasonic mixing was achieved using a Branson sonifier 550 equipped with a 3 mm tapered microtip (300 ms/s pulses, Output power 50%). Photo-polymerization experiments are carried out using a 40 W low-pressure mercury UV lamp (Heraeus) emitting at a wavelength of 254 nm. For HRSTEM experiments, a Titan-G2 probe corrected STEM was used to study the Ru/Rh repartition on the carbon nanotubes. The emitted X-rays were collected by the four detectors with a 0.7 steradian collecting angle. The probe was smaller than 2 Å and its current was almost 250 pA. K-Lines were used to distinguish Ru and Rh as illustrated in Figure S1. XPS analysis was carried out with an Escalab 250 XI spectrometer (Thermo Fisher Scientific Inc.) using a monochromatic Al Kα source (1486.7 eV). The X-ray spot diameter was » 900 µm. For the non-conductive samples, the analysis was carried out using a charge compensation flood gun. The pass energy for high-resolution spectra reported in the following was 20 eV. The data processing was performed using Avantage software (Thermo Fisher Scientific Inc.). The C-1s signal for adventitious carbon was used to correct the charge effect. The C–C/C–H component of C-1s spectra was fixed at 285.0 eV. The background from each spectrum was subtracted using a Shirley-type background. Multi-walled carbon nanotubes (MWCNTs), prepared by catalytic decomposition of methane according to the previously reported method,[1] were obtained from the Department of Chemistry and State Key Laboratory of Physical Chemistry for the Solid Surface, Xiamen University, China.

2. Ru-Rh particle synthesis

The synthesis of nanoparticles was achieved using a previously reported procedure (*Chem. Mater.*, 2000, **12**, 1622). A solution of $RhCl_3{\cdot}3H_2O$ (39.5 mg, 0.15 mmol) and $RuCl_3{\cdot}6H_2O$ (47.5 mg, 0.15 mmol) in water (5 mL) was mixed with ethylene glycol (100 mL). An aqueous solution of NaOH 0.5 M (5 mL) was added to the stirred mixture and the reaction was heated to 160 °C. After 3 h, a stable transparent brown homogeneous colloid of Ru-Rh NPs was formed.

3. Assembly of Ru-Rh nanoparticles on carbon nanotubes

The assembly of Ru-Rh nanoparticles at the surface of carbon nanotubes was achieved according to our previously reported procedure (*Angew. Chem. Int. Ed.*, 2011, **50**, 7533).

4. Spectroscopic data

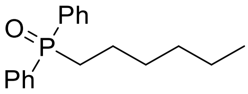

3a

Spectral data in agreement with previous reports from the literature:[2]

^{1}H-NMR (400 MHz, $CDCl_3$): *δ* 0.88 (t, 3H), 1.24–1.27 (m, 4H), 1.40 (m, 2H), 1.62 (m, 2H), 7.44–7.54 (m, 6H, ArH), 7.72–7.77 ppm (m, 4H, ArH).

^{13}C-NMR (100 MHz, $CDCl_3$): *δ* 14.0, 21.4, 22.4, 29.7 (d), 30.6, 31.3, 128.5 (4C), 130.7 (4C), 131.6 (2C), 133.5 (2C, d) ppm.

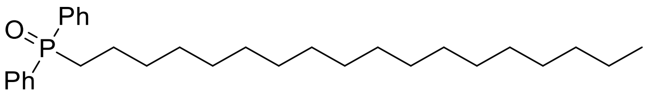

3b

Spectral data in agreement with previous reports from the literature:[3]

^{1}H-NMR (400 MHz, $CDCl_3$): *δ* 0.89 (t, 3H), 1.23–1.31 (m, 28H), 1.40 (m, 2H), 1.62 (m, 2H), 2.20–2.30 (m, 2H), 7.44–7.54 (m, 6H, ArH), 7.72–7.77 ppm (m, 4H, ArH).

^{13}C-NMR (100 MHz, $CDCl_3$): *δ* 14.1, 21.4, 22.7, 29.0–29.7 (13C), 30.5 (d), 31.9, 128.5 (4C), 130.8 (4C), 131.6 (2C), 133.2 (2C, d) ppm.

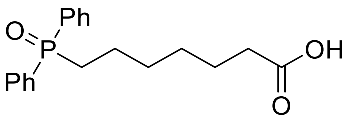

3c

^{1}H-NMR (400 MHz, $CDCl_3$): *δ* 1.03–1.61 (m, 8H), 2.05–2.27 (m, 4H), 7.38–7.47 (m, 6H, ArH), 7.66–7.71 (m, 4H, ArH), 9.22 ppm (br s, 1H).

^{13}C-NMR (100 MHz, $CDCl_3$): *δ* 21.15, 25.1, 28.6, 29.3 (d), 30.4, 35.8, 128.6 (4C), 130.8 (4C), 131.7 (2C), 132.9 (2C, d), 179.6 ppm.

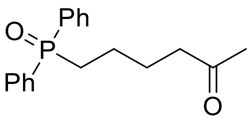

3d

^{1}H-NMR (400 MHz, $CDCl_3$): *δ* 1.58–1.70 (m, 4H), 2.7 (s, 3H), 2.22-2.29 (m, 2H), 7.42–7.52 (m, 6H, ArH), 7.68–7.74 ppm (m, 4H, ArH).

^{13}C-NMR (100 MHz, $CDCl_3$): *δ* 21.2, 24.8, 29.5 (d), 30.0, 43.1, 128.6 (4C), 130.7 (4C), 131.7 (2C), 133.0 (2H, d), 208.4 ppm.

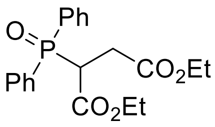

3e

Spectral data in agreement with previous reports from the literature:[4]

^{1}H-NMR (400 MHz, $CDCl_3$): δ 0.86 (m, 3H), 1.18 (m, 1H), 2.71–2.78 (m, 1H), 3.80 (m, 2H), 4.01 (m, 3H), 7.46–7.57 (m, 6H, ArH), 7.81–7.88 ppm (m, 4H, ArH).

^{13}C-NMR (100 MHz, $CDCl_3$): δ 13.5, 14.1, 30.8, 44.6 (d), 61.2, 61.5, 128.7 (4C), 130.0 (2C, d), 131.5 (4C), 132.5 (2C), 168.6, 171.4 ppm.

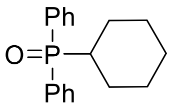

3f

Spectral data in agreement with previous reports from the literature:[5]

^{1}H-NMR (400 MHz, $CDCl_3$): δ 1.19–1.30 (m, 3H), 1.46–1.50 (m, 2H), 1.67–1.80 (m, 5H), 2.17–2.26 (m, 1H), 7.41–7.50 (m, 6H, ArH), 7.74–7.79 ppm (m, 4H, ArH).

^{13}C-NMR (100 MHz, $CDCl_3$): δ 24.8 (2C), 25.8, 26.3 (2C), 37.3 (d), 128.5 (4C), 131.0 (4C), 131.4 (2C), 132.2 (2C, d) ppm.

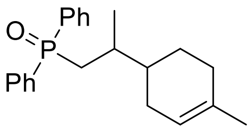

3g

This product was obtained as a 1:1 mixture of 2 diastereoisomers.

^{1}H-NMR (400 MHz, $CDCl_3$): δ 0.97–1.0 (m, 3H), 1.16–1.28 (m, 2H), 1.44–2.15 (m, 10H), 2.36 (m, 1H), 5.32 (s, 1H), 7.46–7.50 (m, 6H, ArH), 7.73–7.77 ppm (m, 4H, ArH).

^{13}C-NMR (100 MHz, $CDCl_3$): δ 17.7, 18.1, 23.4, 25.3, 26.4, 27.4, 28.5, 30.6, 32.0, 33.4, 33.7, 34.1, 34.4, 40.1, 120.4, 130.8, 131.5, 134.0 ppm.

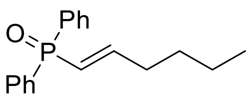

3h

Spectral data in agreement with previous reports from the literature:[6]

^{1}H-NMR (400 MHz, $CDCl_3$): δ 0.86 (m, 3H), 1.18 (m, 1H), 1.35 (m, 2H), 2.52 (m, 2H), 6.09 (m, 1H), 6.70 (m, 1H), 7.42–7.50 (m, 6H, ArH), 7.50–7.76 ppm (m, 4H, ArH).

^{13}C-NMR (100 MHz, $CDCl_3$): δ 13.8, 22.2, 30.7, 31.0, 121.3 (d), 128.5 (4C), 130.9 (4C), 131.5 (2C), 134.7 (2C, d), 155.1 ppm.

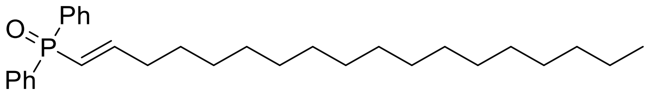

3i

^{1}H-NMR (400 MHz, $CDCl_3$): δ 0.88 (m, 3H), 1.19–1.37 (m, 28H), 2.51 (m, 2H), 6.11 (m, 1H), 6.74 (m, 1H), 7.44–7.53 (m, 6H, ArH), 7.74–7.78 ppm (m, 4H, ArH).

^{13}C-NMR (100 MHz, $CDCl_3$): δ 14.1, 22.7, 28.8–29.7 (11C), 30.9, 31.0, 31.9, 121.2 (d), 128.5 (4C) 130.9 (4C), 131.5 (2C), 134.6 (2C, d), 155.3 ppm.

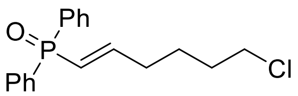

3j

Spectral data in agreement with previous reports from the literature:[7]

^{1}H-NMR (400 MHz, $CDCl_3$): δ 1.49–1.57 (m, 2H), 1.66–1.73 (m, 2H), 3.46 (t, 2H), 6.13 (m, 1H), 6.68 (m, 1H), 7.43–7.52 (m, 6H, ArH), 7.71–7.75 ppm (m, 4H, ArH).

^{13}C-NMR (100 MHz, $CDCl_3$): δ 26.0, 29.9, 31.9, 44.8, 122.1 (d), 128.6 (4C), 130.9 (4C), 131.6 (2C), 134.4 (2C, d), 154.0 ppm.

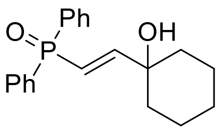

3k

Spectral data in agreement with previous reports from the literature:[8]

^{1}H-NMR (400 MHz, $CDCl_3$): δ 1.22 (m, 1H), 1.43–1.84 (m, 10H), 5.93 (m, 1H), 6.24 (s, 1H), 6.88 (m, 1H), 7.43–7.51 (m, 6H, ArH), 7.68–7.73 ppm (m, 4H, ArH).

^{13}C-NMR (100 MHz, $CDCl_3$): δ 21.7, 25.5, 38.0, 71.8, 118.1 (d), 128.6 (4C), 131.2 (4C), 131.9 (2C) 133.0 (2C, d), 162.3 ppm.

5. Copies of NMR spectra

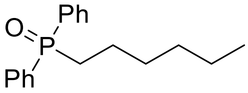

3a

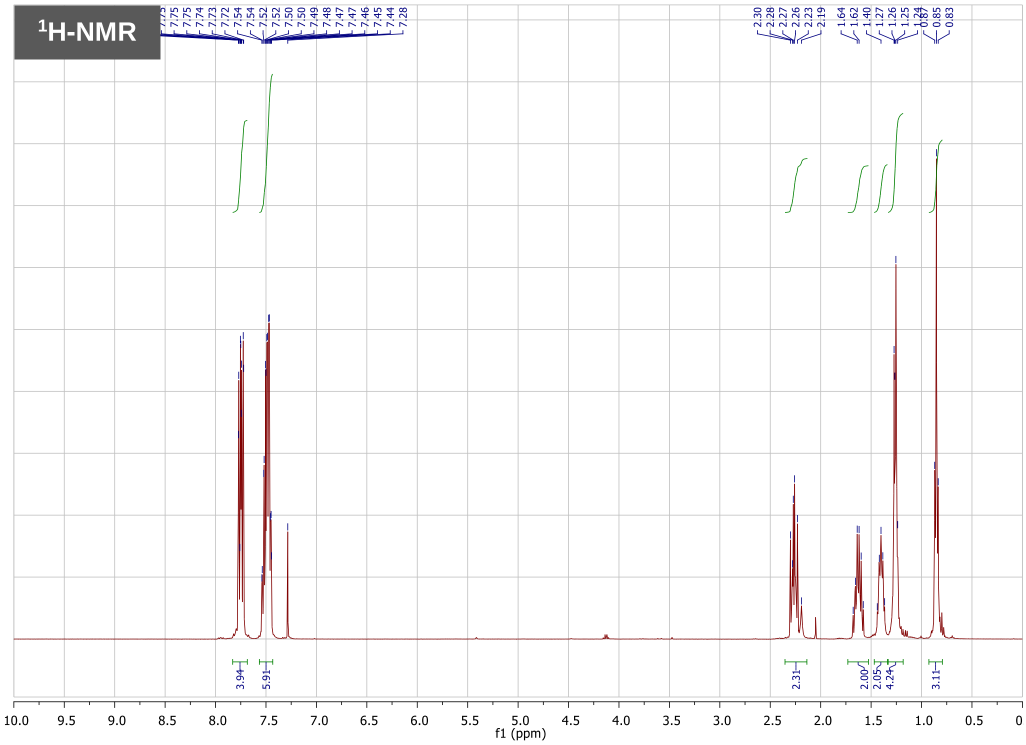

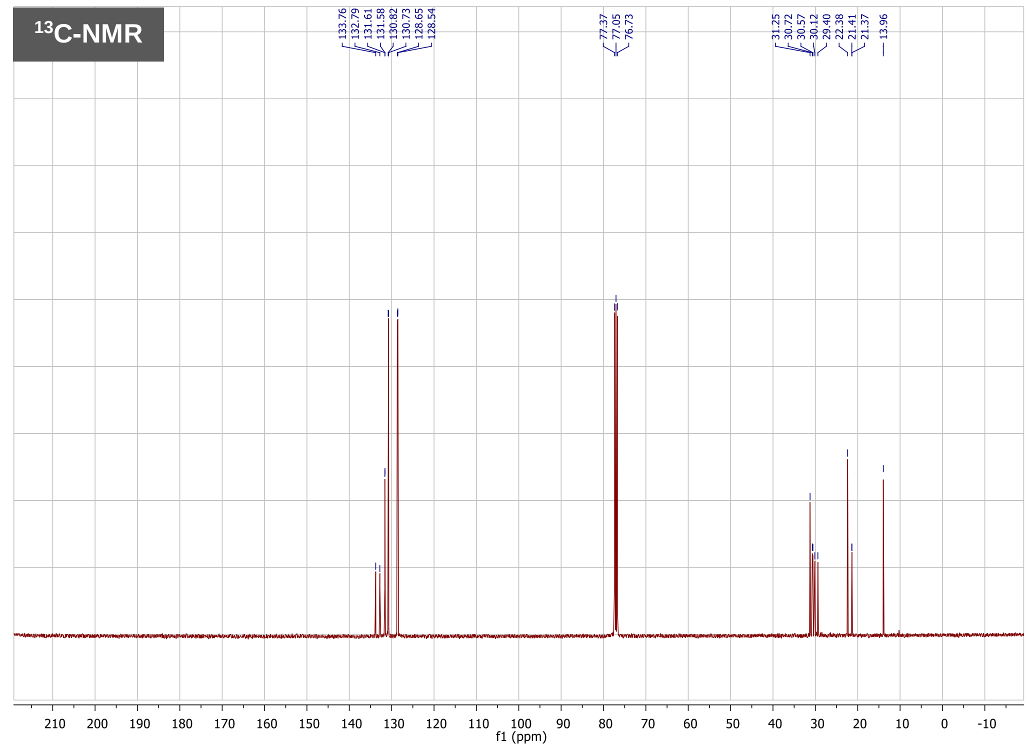

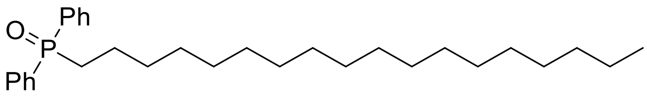
O
P
Ph
Ph

3b

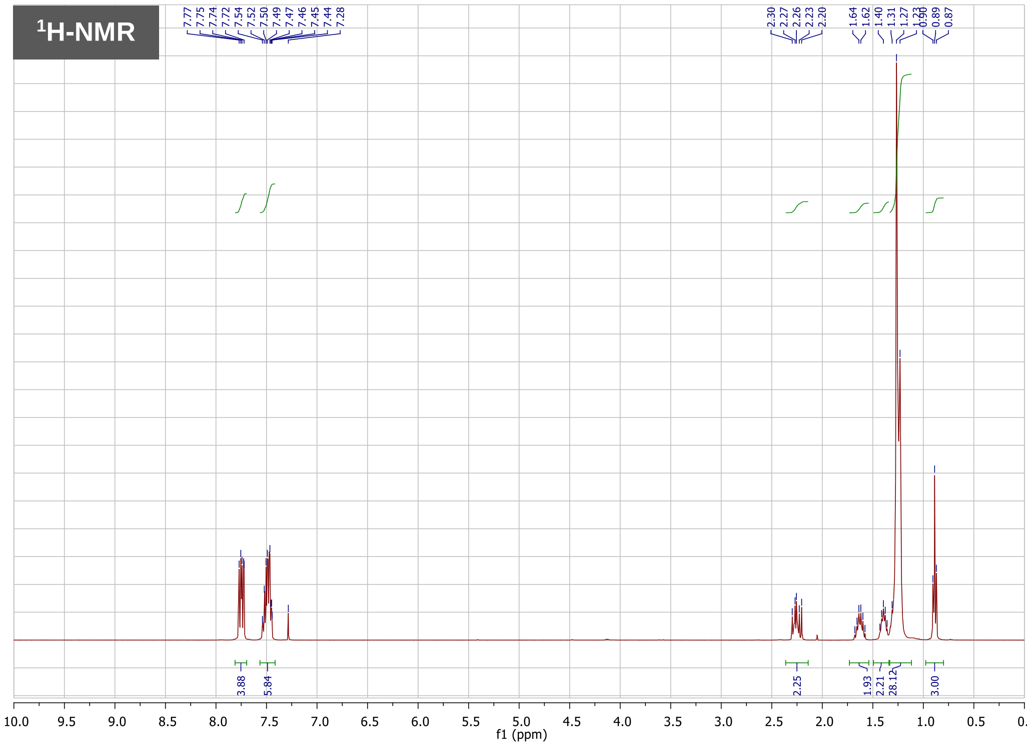
1H-NMR
7.77 7.75 7.74 7.72 7.54 7.52 7.50 7.49 7.47 7.46 7.45 7.44 7.28
2.30 2.27 2.26 2.23 2.20
1.64 1.62 1.40 1.31 1.27 1.23 0.90 0.89 0.87
3.88 5.84 2.25 1.93 2.21 28.12 3.00
f1 (ppm)

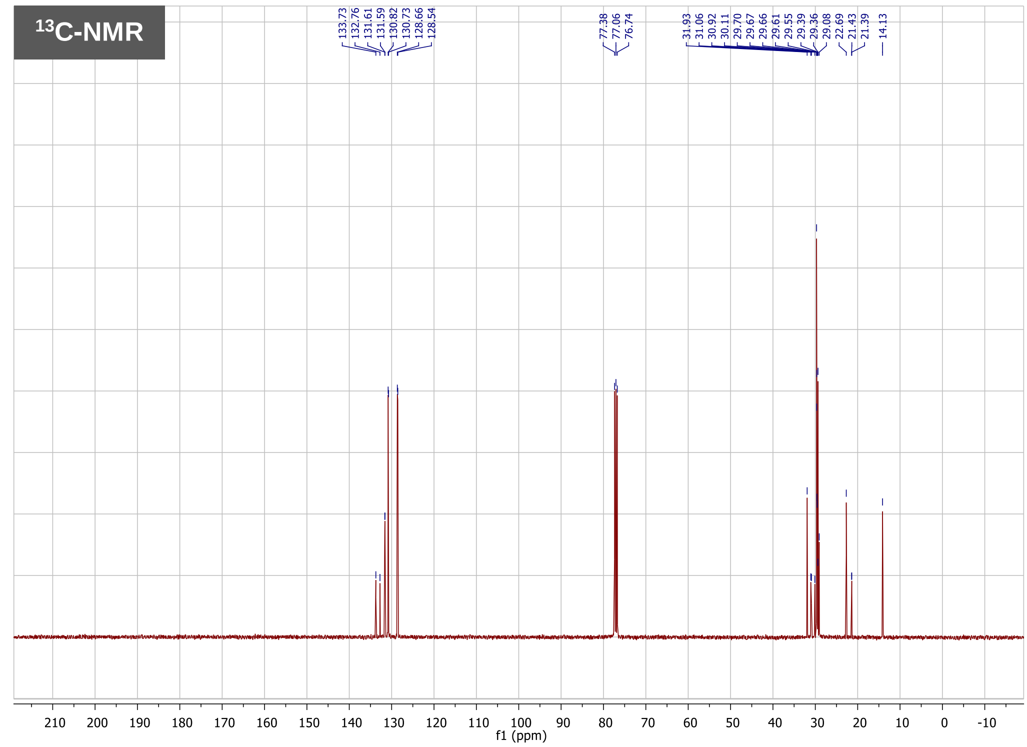
13C-NMR
133.73 132.76 131.61 131.59 130.82 130.73 128.66 128.54
77.38 77.06 76.74
31.93 31.06 30.92 30.11 29.70 29.67 29.66 29.61 29.55 29.39 29.36 29.08 22.69 21.43 21.39 14.13
f1 (ppm)

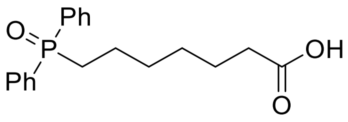

3c

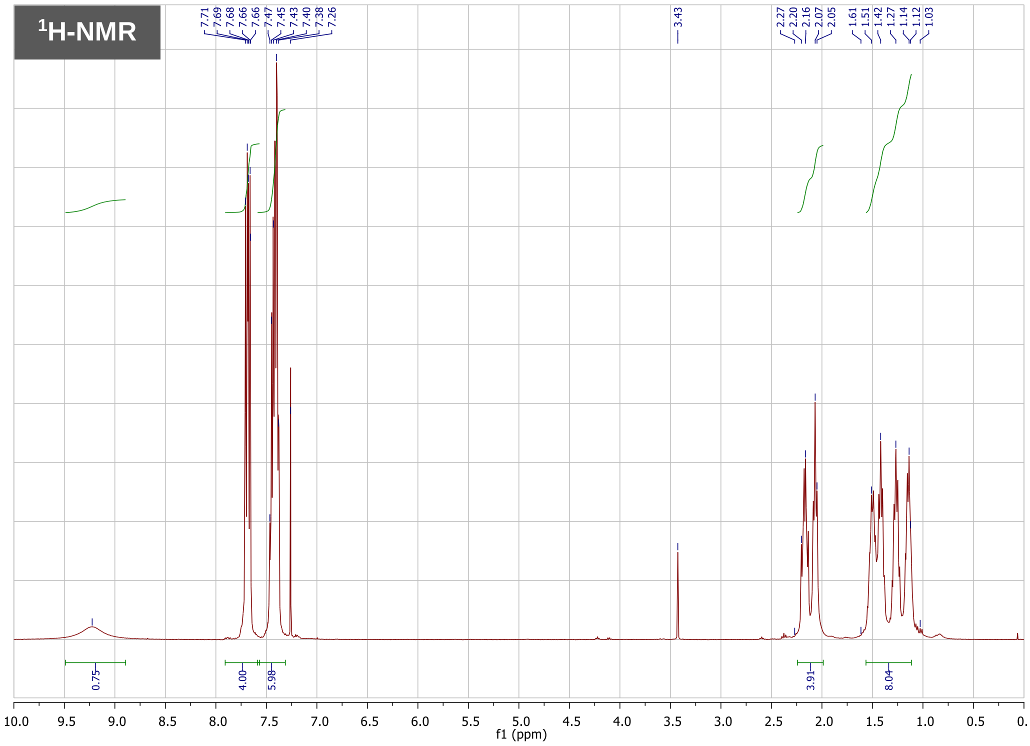

1H-NMR
7.71
7.69
7.68
7.66
7.66
7.47
7.45
7.43
7.40
7.38
7.26
3.43
2.27
2.20
2.16
2.07
2.05
1.61
1.51
1.42
1.27
1.14
1.12
1.03
0.75
4.00
5.98
3.91
8.04
f1 (ppm)

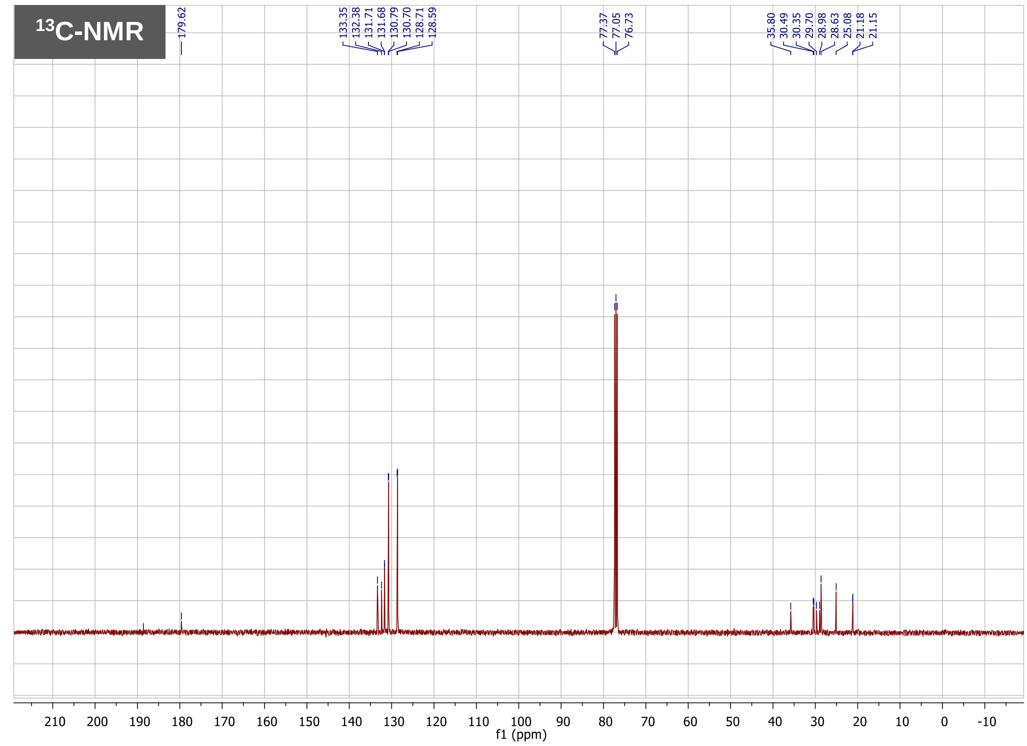

13C-NMR
179.62
133.35
132.38
131.71
131.68
130.79
130.70
128.71
128.59
77.37
77.05
76.73
35.80
30.49
30.35
29.70
28.98
28.63
25.08
21.18
21.15
f1 (ppm)

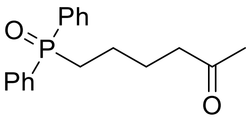

3d

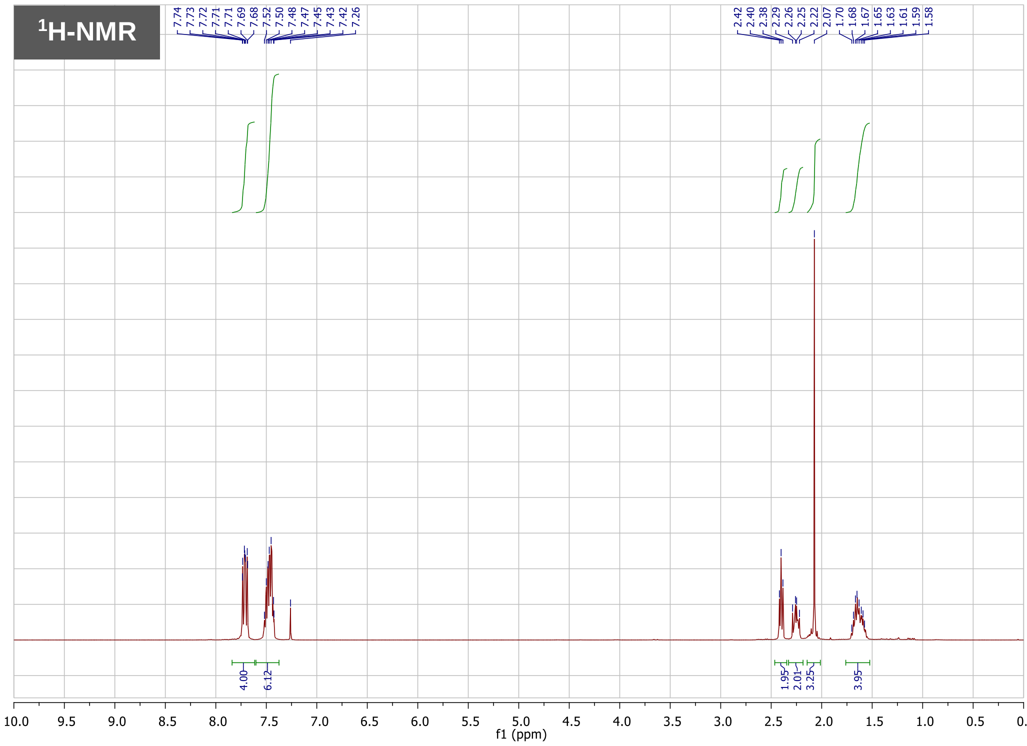

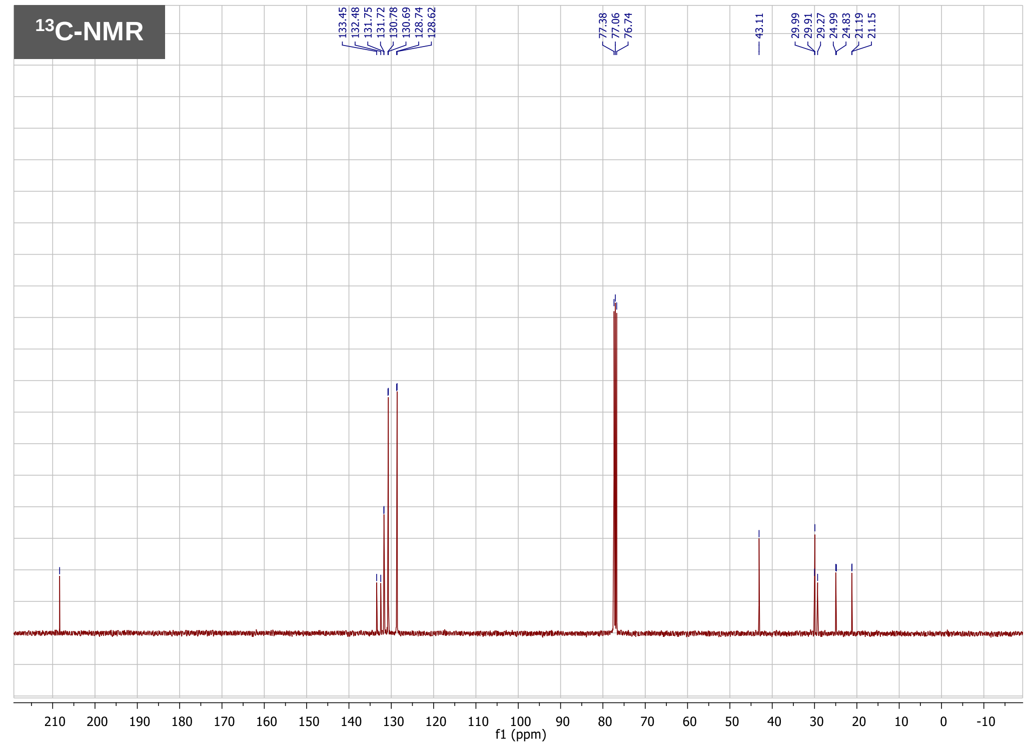

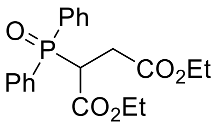

3e

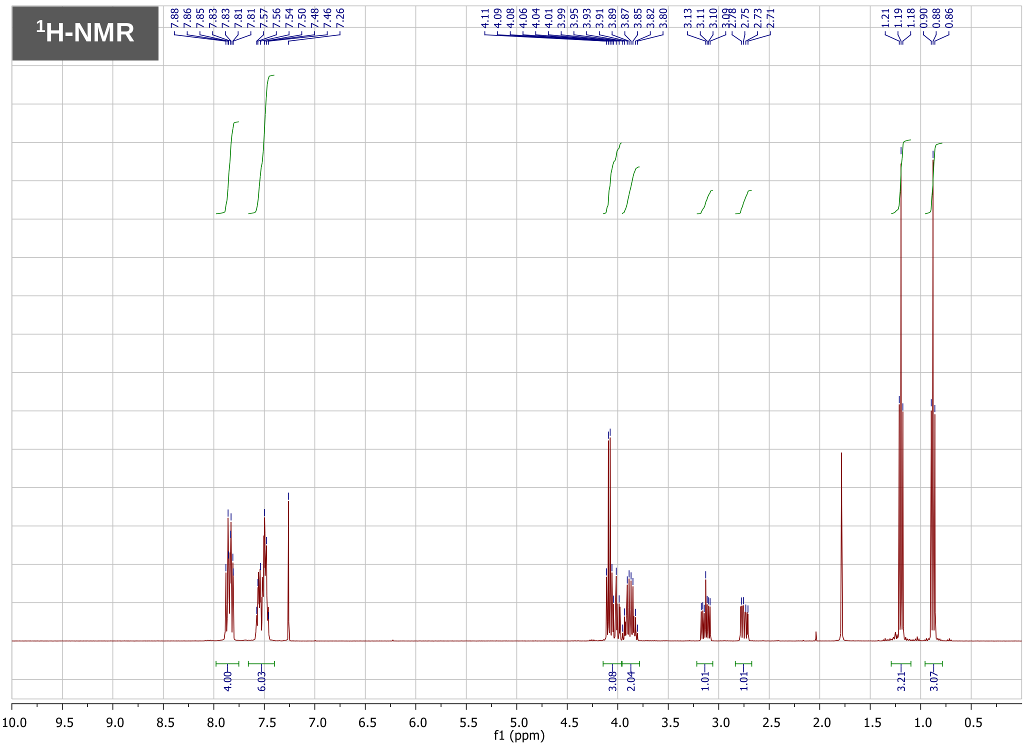

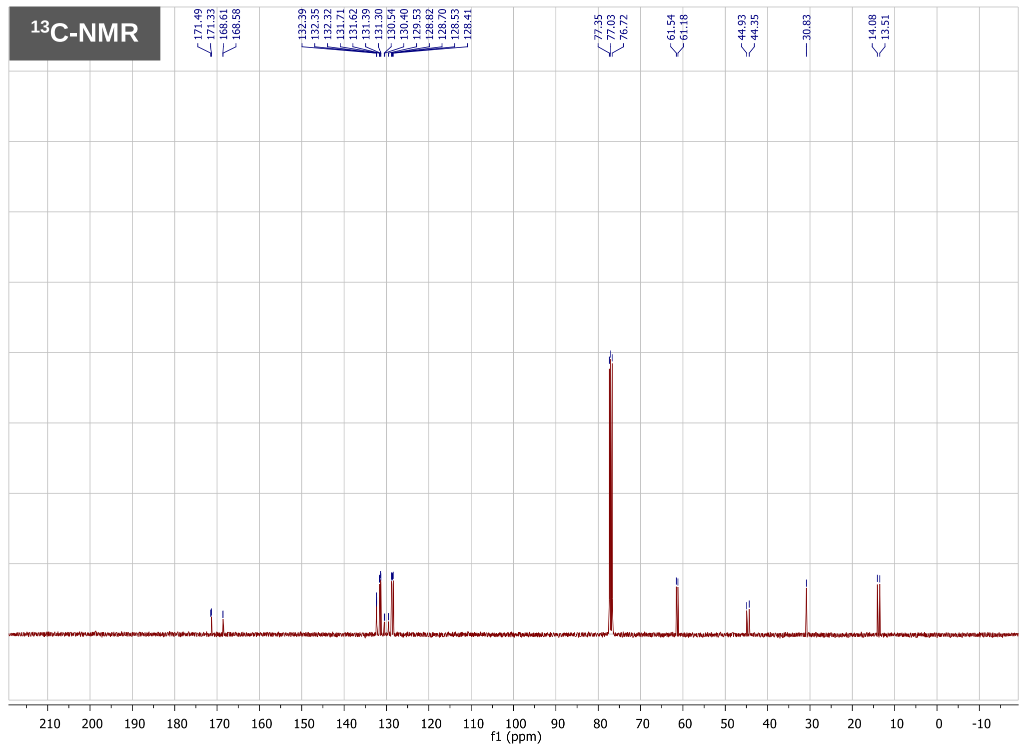

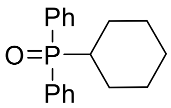

3f

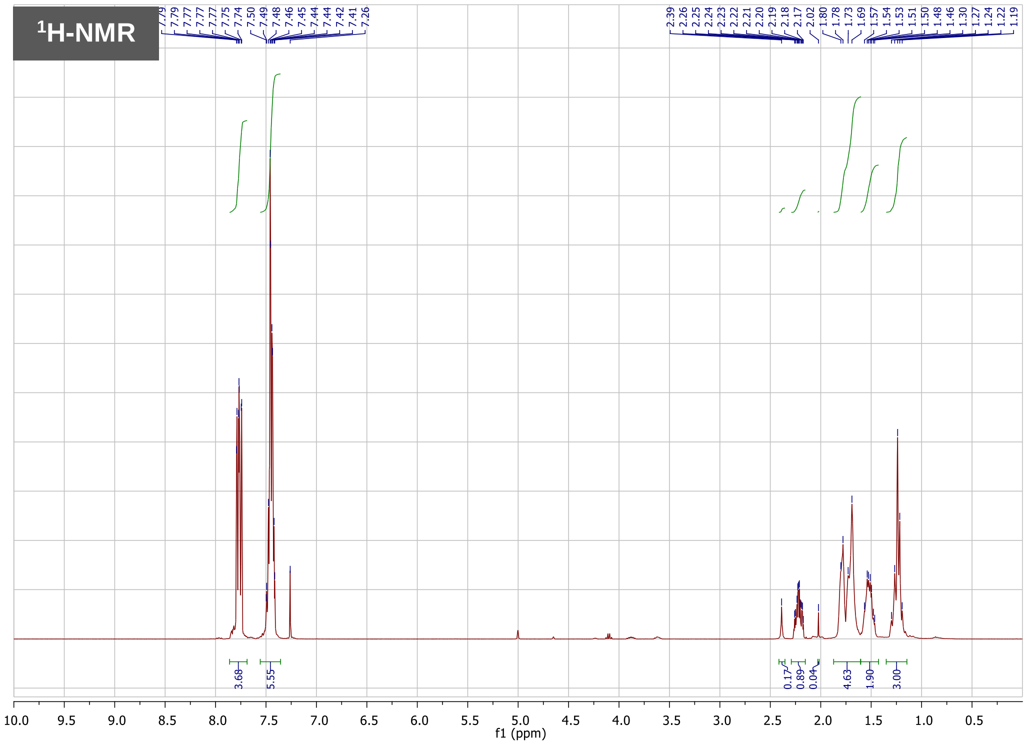

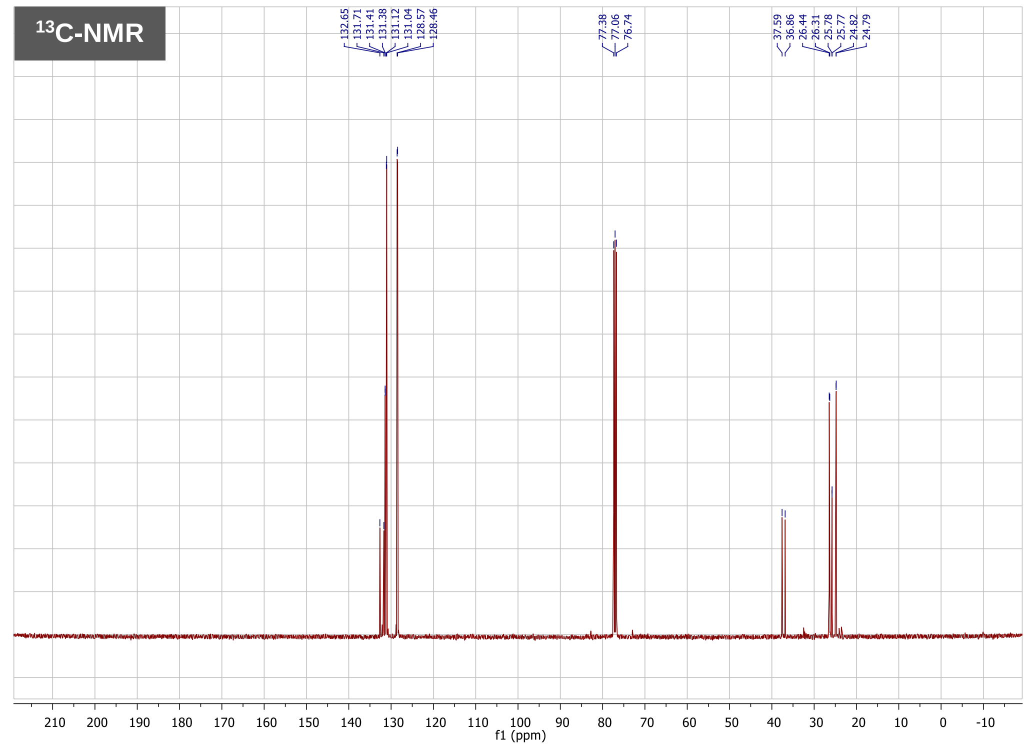

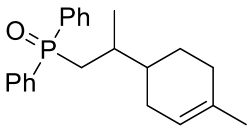
O
P
Ph
Ph

3g

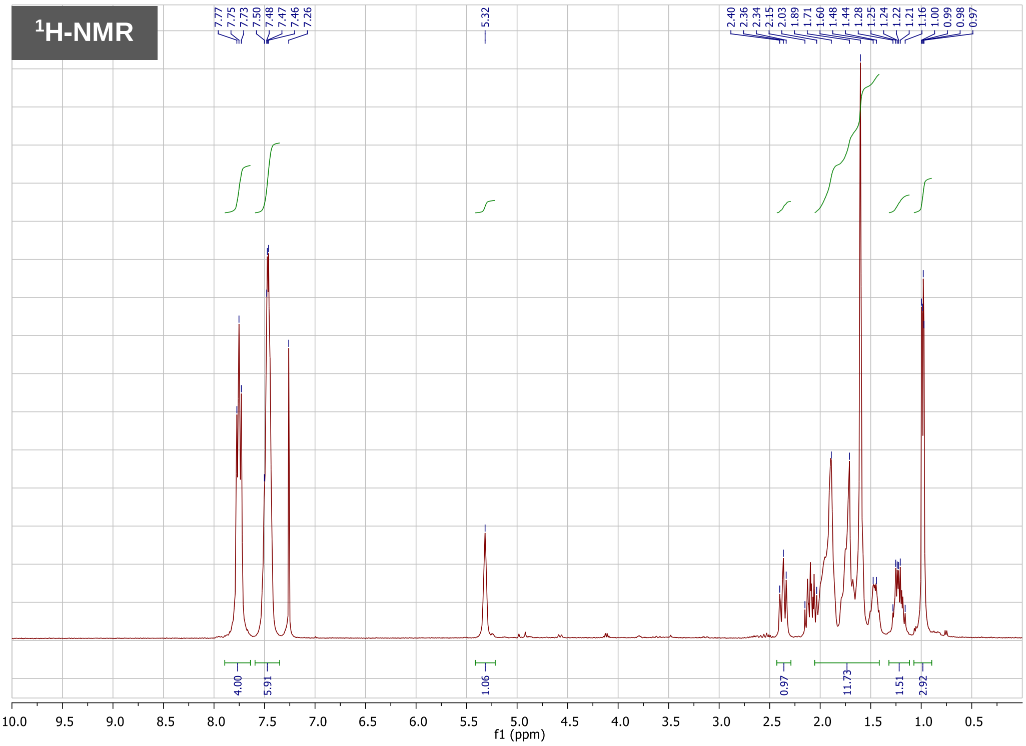
1H-NMR
7.77
7.75
7.73
7.50
7.48
7.47
7.46
7.26
5.32
2.40
2.36
2.34
2.15
2.03
1.89
1.71
1.60
1.48
1.44
1.28
1.25
1.24
1.22
1.21
1.16
1.00
0.99
0.98
0.97
4.00
5.91
1.06
0.97
11.73
1.51
2.92
f1 (ppm)

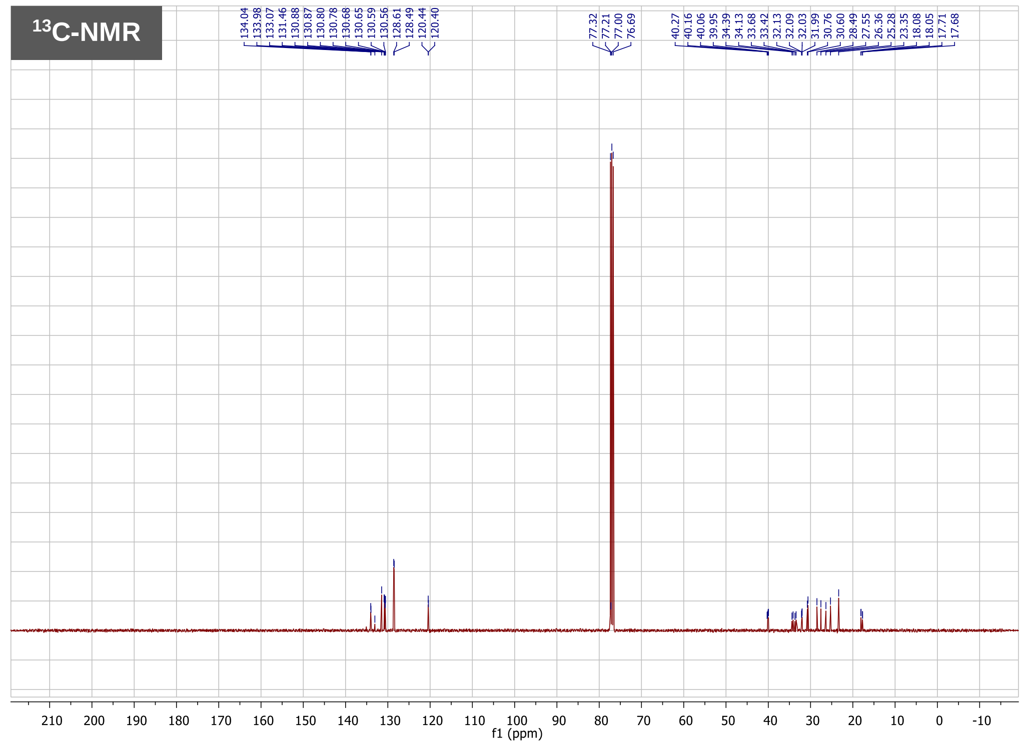
13C-NMR
134.04
133.98
133.07
131.46
130.88
130.87
130.80
130.78
130.68
130.65
130.59
130.56
128.61
128.49
120.44
120.40
77.32
77.21
77.00
76.69
40.27
40.16
40.06
39.95
34.39
34.13
33.68
33.42
32.13
32.09
32.03
31.99
30.76
30.60
28.49
27.55
26.36
25.28
23.35
18.08
18.05
17.71
17.68
f1 (ppm)

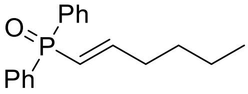

3h

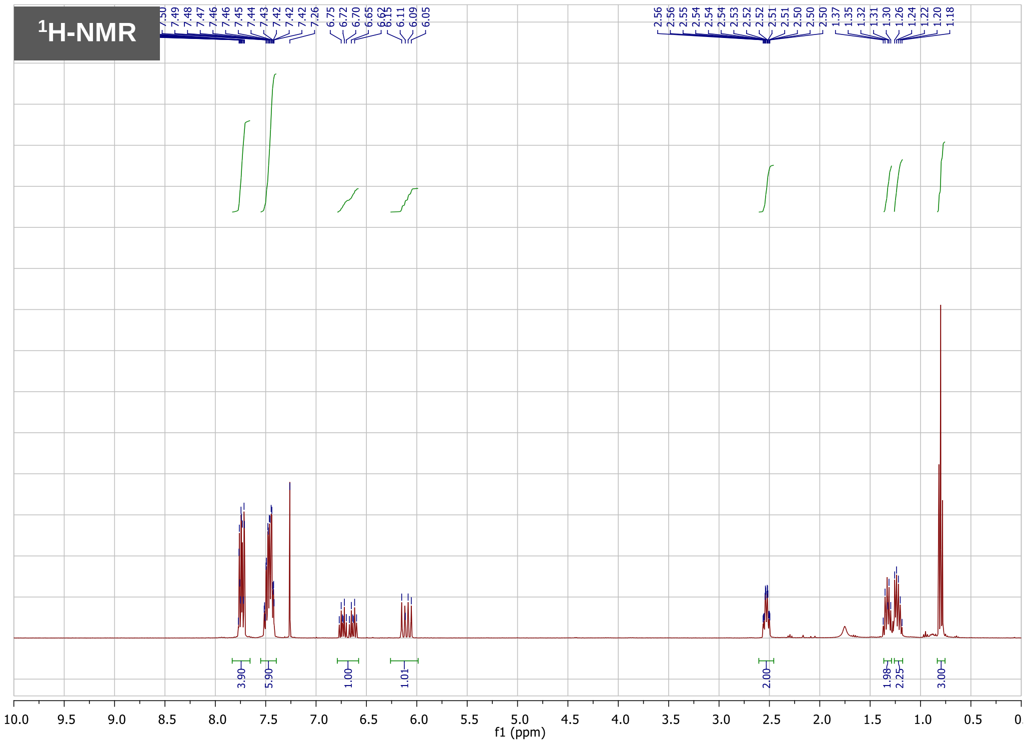

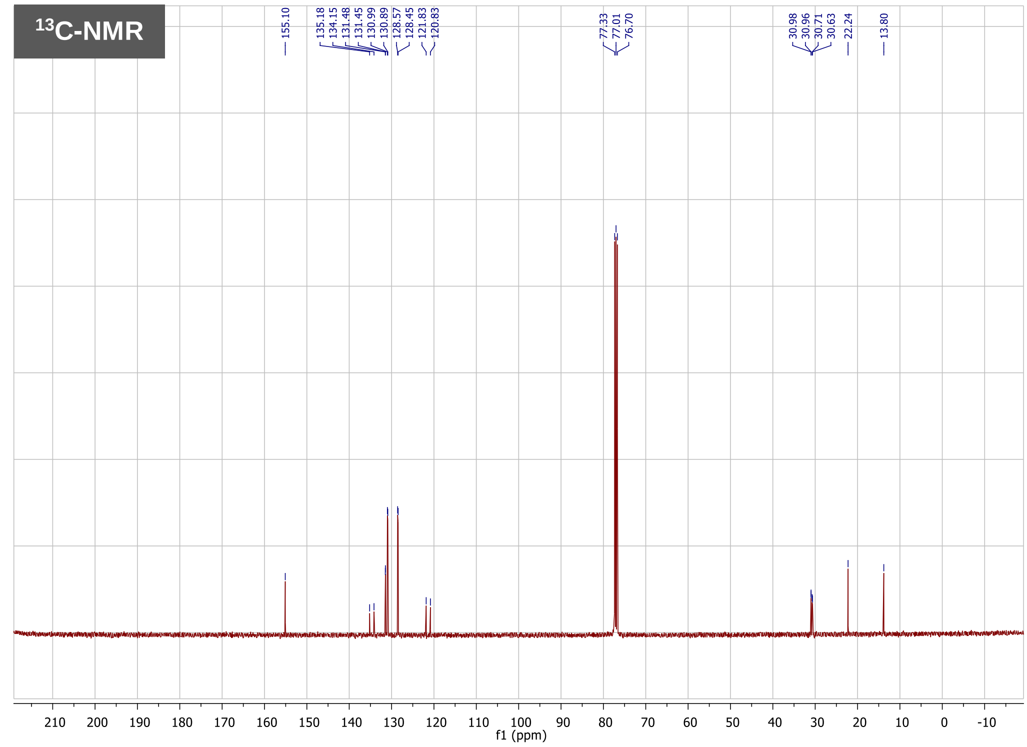

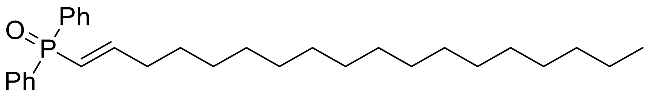

3i

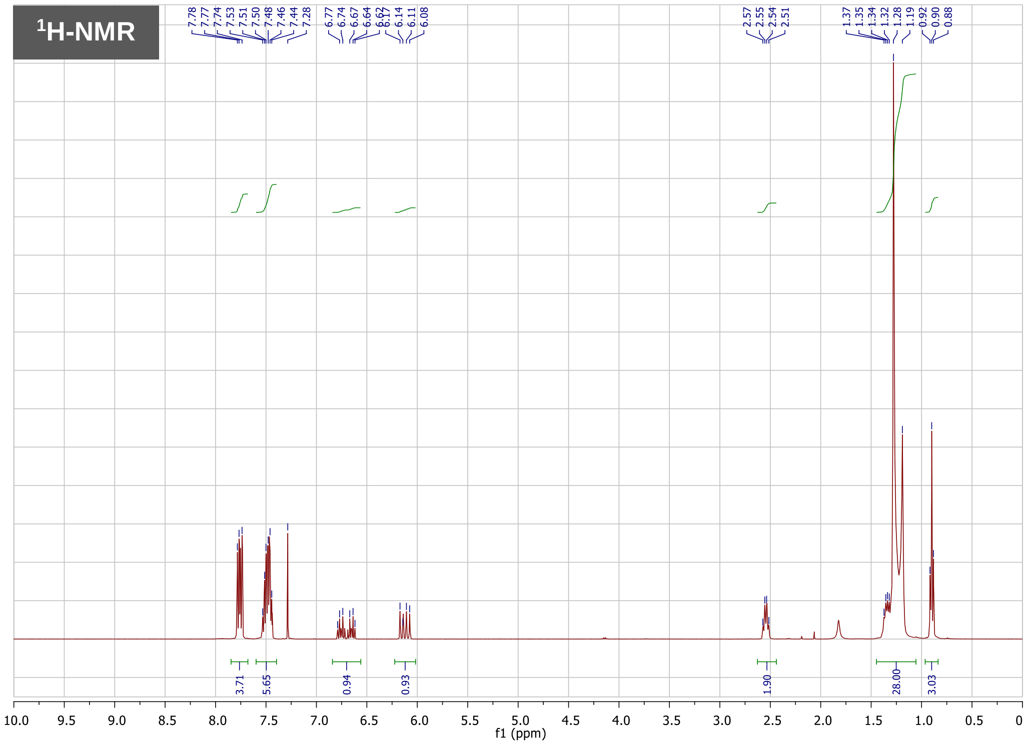

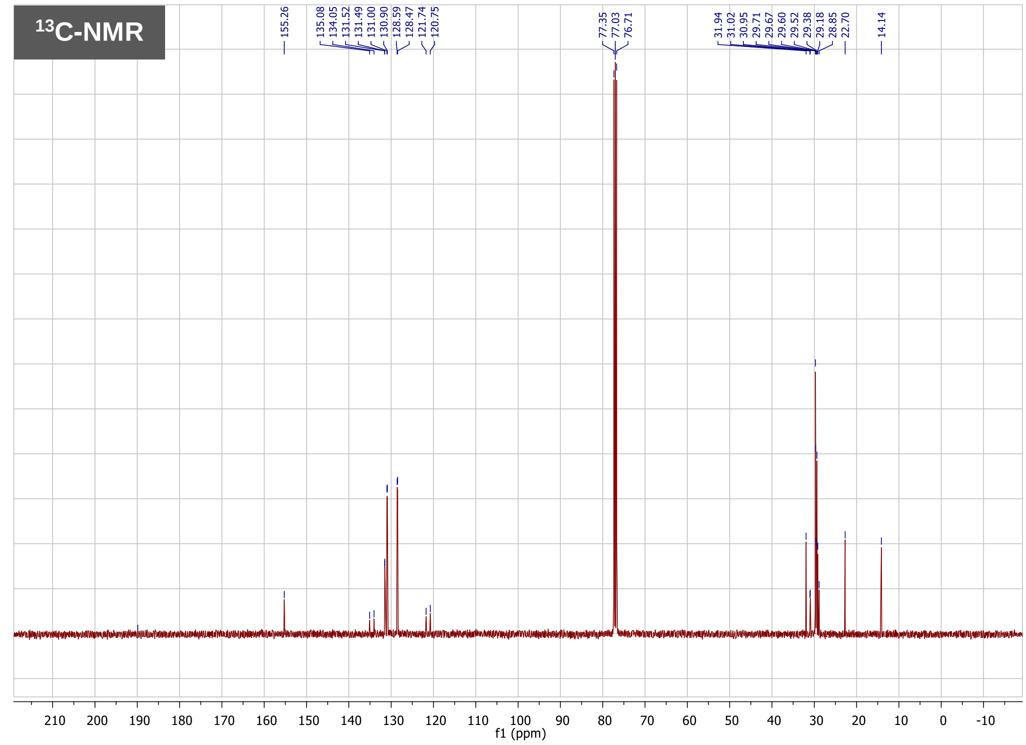

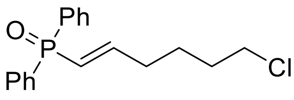
O
P
Ph
Ph
Cl

3j

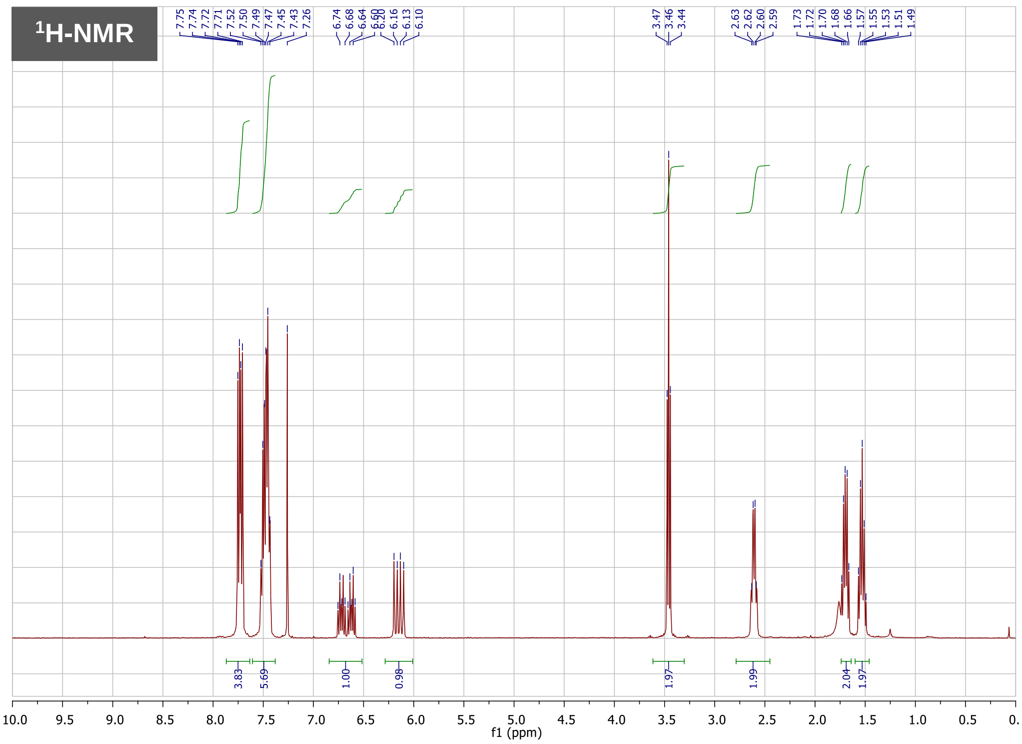
1H-NMR
7.75
7.74
7.72
7.71
7.52
7.50
7.49
7.47
7.45
7.43
7.26
6.74
6.68
6.64
6.58
6.16
6.13
6.10
3.47
3.46
3.44
2.63
2.62
2.60
2.59
1.73
1.72
1.70
1.68
1.66
1.57
1.55
1.53
1.51
1.49
3.83
5.69
1.00
0.98
1.97
1.99
2.04
1.97
f1 (ppm)

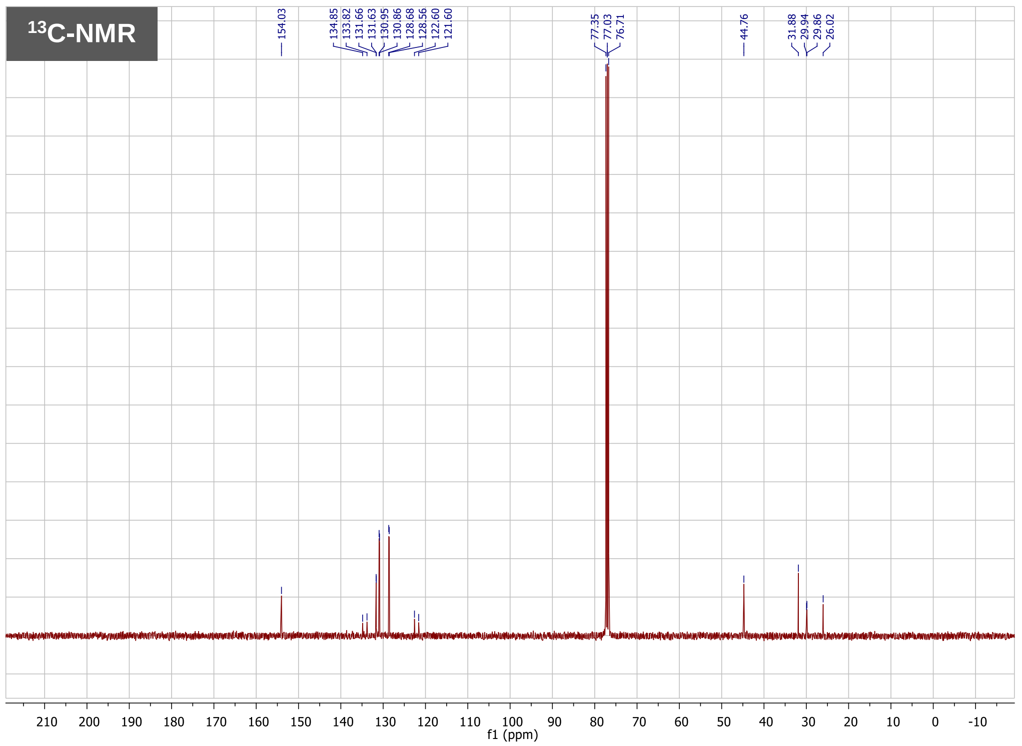
13C-NMR
154.03
134.85
133.82
131.66
131.63
130.95
130.86
128.68
128.56
122.60
121.60
77.35
77.03
76.71
44.76
31.88
29.94
29.86
26.02
f1 (ppm)

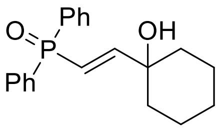

3k

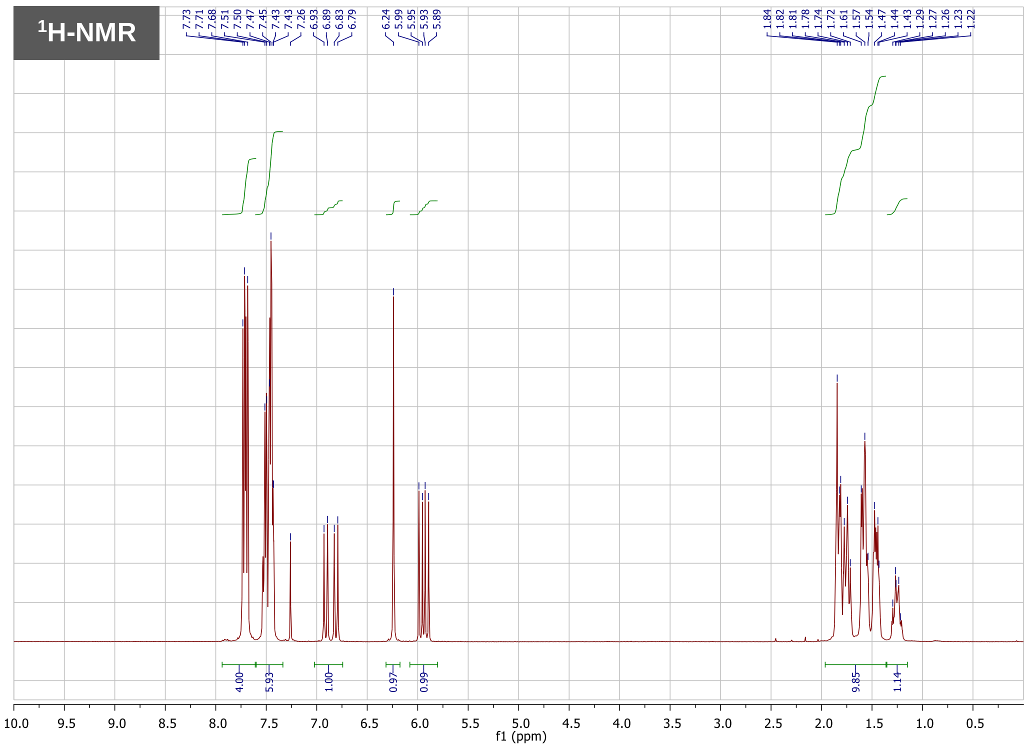

1H-NMR
7.73
7.71
7.68
7.51
7.50
7.47
7.45
7.43
7.43
7.26
6.93
6.89
6.83
6.79
6.24
5.99
5.95
5.93
5.89
1.84
1.82
1.81
1.78
1.74
1.72
1.61
1.57
1.57
1.54
1.47
1.44
1.43
1.29
1.27
1.26
1.23
1.22
4.00
5.93
1.00
0.97
0.99
9.85
1.14
f1 (ppm)

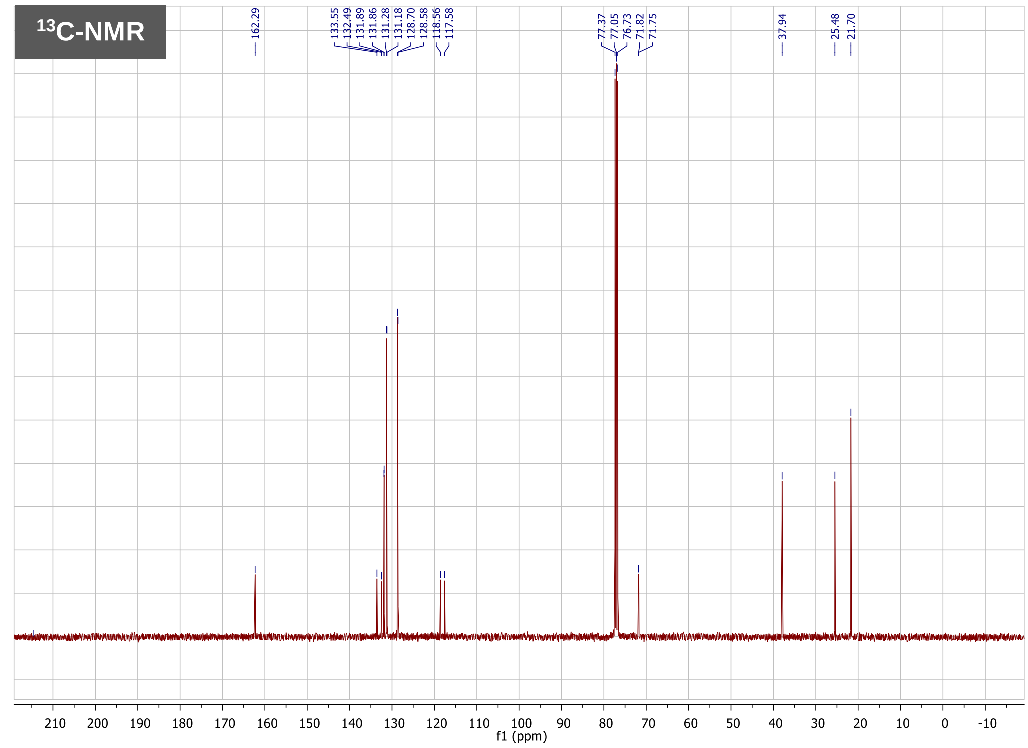

13C-NMR
162.29
133.55
132.49
131.89
131.86
131.28
131.18
128.70
128.58
118.56
117.58
77.37
77.05
76.73
71.82
71.75
37.94
25.48
21.70
f1 (ppm)

6. Supplementary Figures

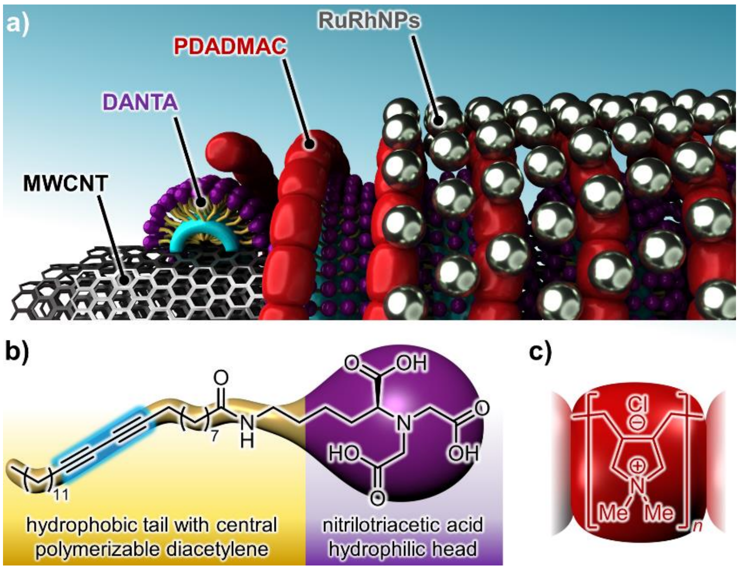

Figure S1. a) General overview of the nanohybrid; b) Structure of DANTA; c) Structure of PDADMAC.

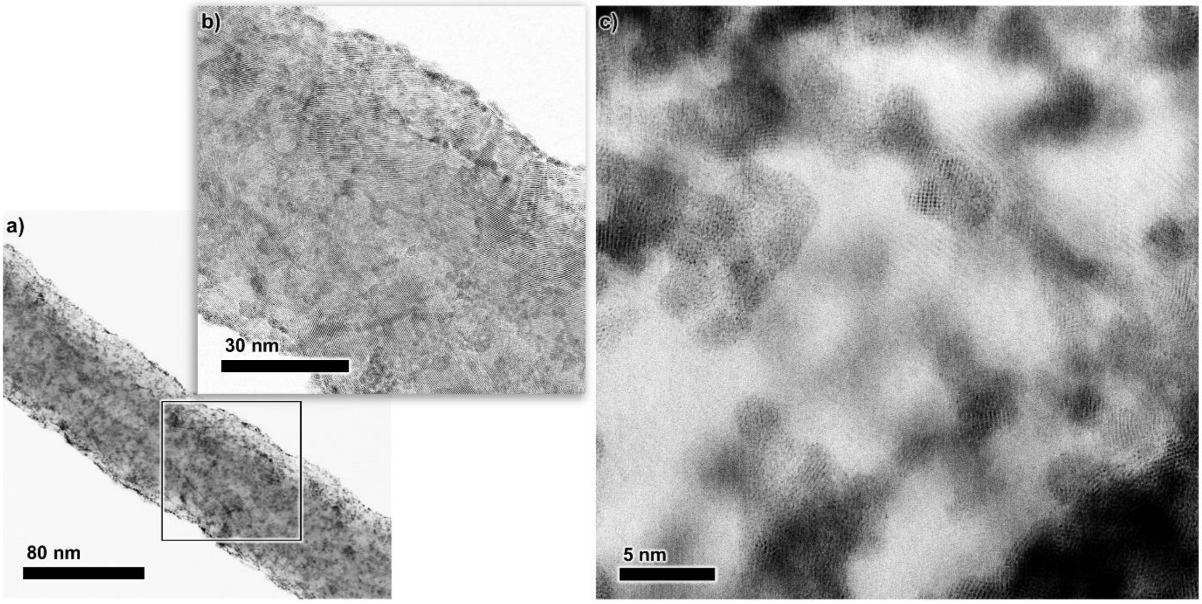

Figure S2. HRTEM images of the RuRhCNT hybrid.

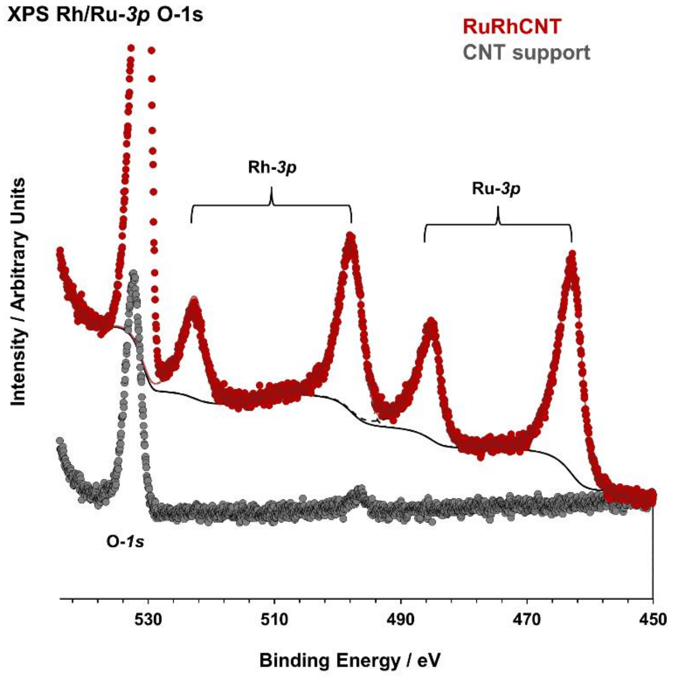

Figure S3. XPS spectrum showing Rh-*3p*, Ru-*3p* and O-*1s* regions for the nanotube support without metals (grey dots) and the RuRhCNT catalyst (red dots).

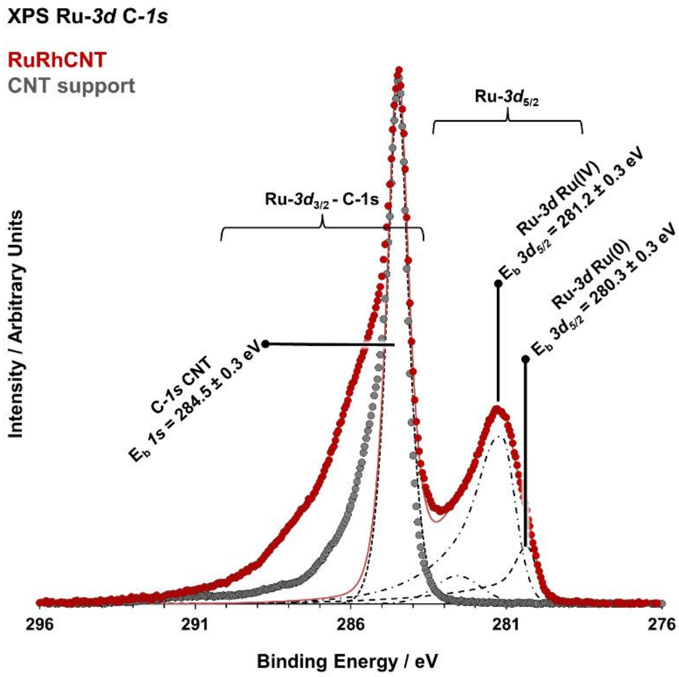

Figure S4. XPS spectrum highlighting the Ru(0) and Ru(IV) contributions (Ru-*3d* region) for the nanotube support without metals (grey dots) and the RuRhCNT catalyst (red dots).

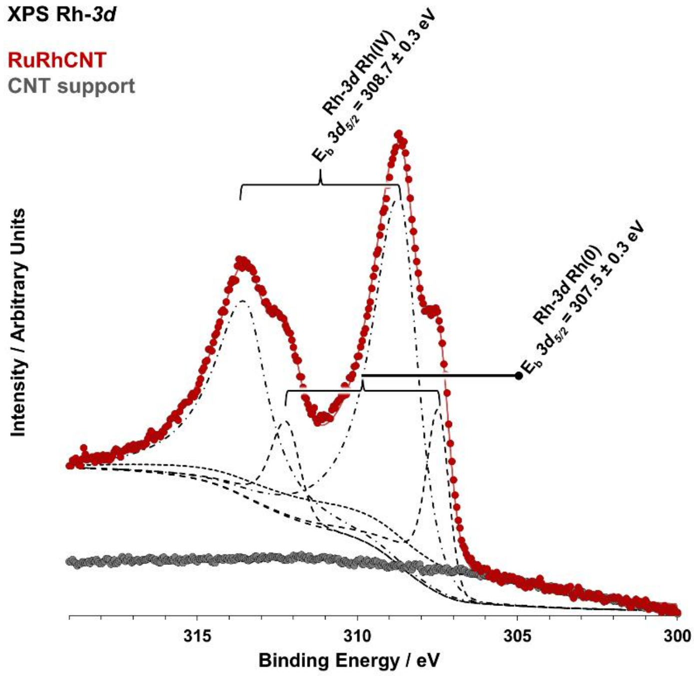

Figure S5. XPS spectrum highlighting the Rh(0) and Rh(IV) contributions (Rh-*3d* region) for the nanotube support without metals (grey dots) and the RuRhCNT catalyst (red dots).

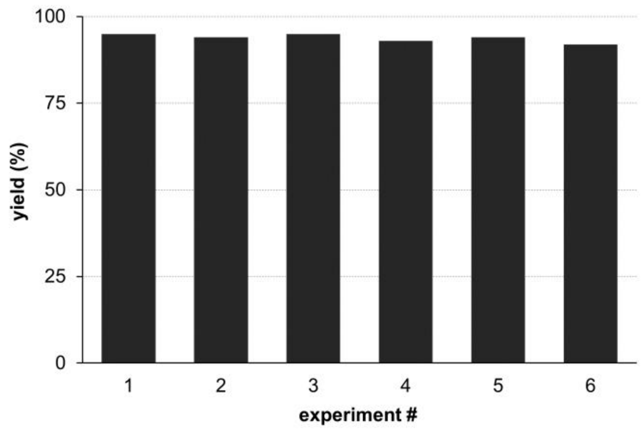

Figure S6. Recycling experiments.

7. References

[1] P. Chen, H.-B. Zhang, G.-D. Lin, Q. Hong and K. R. Tsai, *Carbon*, 1997, **35**, 1495.
[2] Y. Shi, R. Chen, K. Guo, F. Meng, S. Cao, C. Gu and Y. Zhu, *Tetrahedron Lett.*, 2018, **59**, 2062.
[3] A. M. Kawaoka and T. J. Marks, *J. Am. Chem. Soc.*, 2005, **127**, 6311.
[4] Z. Huang, W. Liu, S. Li, Y. Yang, S. Guo and H. Cai, *Synlett*, 2020, **31**, 1295.
[5] Q. Chen, J. Zeng, X. Yan, Y. Huang, Z. Du, K. Zhang and C. Wen, *Tetrahedron Lett.*, 2016, **57**, 3379.
[6] P. Cuadrado, A.M. Gonzalez-Nogal and M. A. Sarmentero, *Chem. Eur. J.*, 2004, **10**, 4491.
[7] T. Huang, Y. Saga, H. Guo, A. Yoshimura, A. Ogawa and L.-B. Han, *J. Org. Chem.*, 2018, **83**, 8743.
[8] A. S. Bogachenkov, A. V. Dogadina, V. P. Boyarskiy and A. V. Vasilyev, *Org. Biomol. Chem.*, 2015, **13**, 1333.